A-line: 4D Printing Morphing Linear Composite Structures

Guanyun Wang[1*], **Ye Tao**[2,1*], **Ozguc Bertug Capunaman**[3], **Humphrey Yang**[3], **Lining Yao**[1]
[1] Human-Computer Interaction Institute, Carnegie Mellon University
[2] Zhejiang University
[3] School of Architecture, Carnegie Mellon University
{guanyunw,ytao2,ocapunam,hanliny,liningy}@andrew.cmu.edu

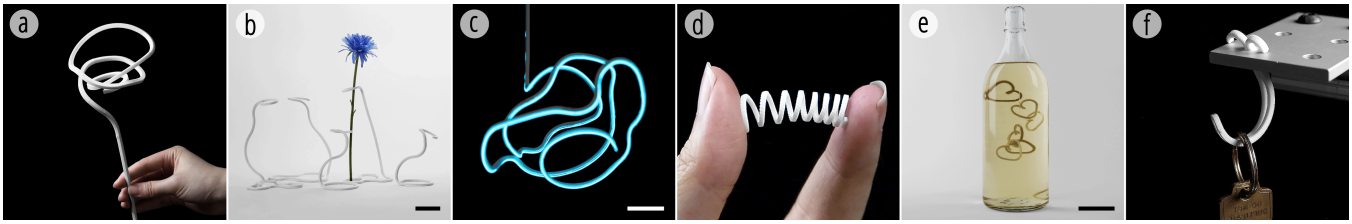

Figure 1: Examples of A-line applications: rose (a), vases (b), lamp (c), compliant mechanisms- spring (d), self-deployable wishing heart (e), and self-locking hook (f). Scale bar: 50mm.

ABSTRACT

This paper presents A-line, a 4D printing system for designing and fabricating morphing three-dimensional shapes out of simple linear elements. In addition to the commonly known benefit of 4D printing to save printing time, printing materials, and packaging space, A-line also takes advantage of the unique properties of thin lines, including their suitability for compliant mechanisms and ability to travel through narrow spaces and self-deploy or self-lock on site. A-line integrates a method of bending angle control in up to eight directions for one printed line segment, using a single type of thermoplastic material. A software platform to support the design, simulation and tool path generation is developed to support the design and manufacturing of various A-line structures. Finally, the design space of A-line is explored through four application areas, including line sculpting, compliant mechanisms, self-deploying, and self-locking structures.

CHI 2019, May 4–9, 2019, Glasgow, Scotland Uk

ACM ISBN 978-1-4503-5970-2/19/05…$15.00
https://doi.org/10.1145/3290605.3300656

CCS CONCEPTS

• **Human-centered computing** → *Interactive systems and tools.*

KEYWORDS

Line-based structure; Line-shaped interface; 4D printing; 3D printing; Self-folding; Morphing; Shape-changing interface.

ACM Reference Format:
Guanyun Wang, Ye Tao, Ozguc Bertug Capunaman, Humphrey Yang, Lining Yao. 2019. A-line: 4D Printing Morphing Linear Composite Structures. In *CHI Conference on Human Factors in Computing Systems Proceedings (CHI 2019), May 4–9, 2019, Glasgow, Scotland Uk.* ACM, New York, NY. 12 pages. DOI: https://doi.org/10.1145/3290605.3300656

1 INTRODUCTION

Line-shaped structures widely exist both in the natural and artificial world. As the basic building components, lines can be observed across scales, from DNA and protein folding mechanisms that construct life at the nano and micro scale, to truss systems at the scale of buildings or bridges. The simplicity of one-dimensionality and the versatile potentials of line folding make line-based construction attractive to different communities, including construction and manufacturing [18], computational graphics [9, 16], the biomedical field [28] and HCI [20, 21]. For instance, lines like tent scaffolds are often easy and space-saving to pack. Lines for chair frames and wire sculptures have their unique aesthetics. Additionally, the inherent mechanical properties of line-based

*The first two authors contributed equally to this work.

structures can be leveraged for compliant mechanisms [15]. Finally, lines have the geometric flexibility to transform into various 2D or 3D geometries in both the man-made and natural world [5, 7, 31].

A-line tries to integrate the aforementioned advantages of line-based structures and to leverage the fact that transformative lines can self-deploy and self-lock. Moreover, A-line adapts an emerging 4D printing technique [1, 32, 35] to simplify its manufacturing process. A-line also offers an inverse design algorithm to simplify its shape design process. In short, by introducing a unique method to compose material, and a tailored algorithm to design the targeted shape, A-line shows how thermoplastic can be printed into a set of straight lines and subsequently triggered to self-fold into targeted wireframe structures in both 2D and 3D. Compared to existing line sculpting methods, which often have very limited functions in CAD tools and require specific machinery or technique (e.g., wire benders for iron wires, and molds for bamboo strings), A-line presents an easy method to design and fabricate line-based structures by leveraging desktop 3D printers.

In this paper, we will first explain the material composition method and mechanism, followed by the workflow and algorithms of the design and simulation software. We will then discuss the triggering conditions and experimental setup, and finally the applications.

2 CONTRIBUTION

The main contributions of this work are as follows:

- Novel composite design method for 4D printing: we present a novel way of fabricating morphing, line-shaped artifacts with hobbyist 3D printers and off-the-shelf thermoplastic printing filaments. The unique linear composite structure enables a single printed line segment to have the capabilities of bending angle control in up to eight directions.
- Customized design tool: we propose a customized design tool to assist users to design, simulate and fabricate.
- Wide design space of linear structures: we explore several line-shaped designs (Figure 1), including self-deployable and self-locking structures, compliant mechanism, space-saving packaging, and line sculpting.

3 RELATED WORK

Customizing 3D Printing

The increasing popularity of 3D printing technology is enabling users to build a personalized world. To adapt 3D printing for customized applications, researchers have developed various 3D printing methods to streamline the design and fabrication process. For instance, a series of projects explored 3D printing metamaterial with mechanical function and tactile feedback [10–12, 19]; some researchers developed multiple methods combining soft fabric with 3D printing [8, 25, 30]; there are additional works merging contemporary 3D printing with hybrid crafting [14, 44]; other researchers focused on producing artifacts with multiple interactive printing techniques [4, 24, 26, 36, 37, 43]. In terms of augmenting an object's physical properties, Medley [3] and ColorMod [27] introduced methods for changing the physical properties and the color of a 3D-printed object during and even after fabrication; 3D Printed Hair [13] and Cilllia [23] augmented artifacts with hair-like structures for tunable frictions. A-line investigates and expands these boundaries by proposing a method which seamlessly combines design with fabrication to 3D print artifacts with a single linear structure.

4D Printing of Morphing Materials and Interfaces

Unlike 3D printing, 4D printing encodes a stimulus response to be triggered after fabrication [17, 29, 32]. While the major design space related to 4D printing in HCI literature [1, 35, 38, 42] has been focused on sheet-like surfaces for shape-changing, flat-packaging, and reducing print time, A-line goes beyond these and explore the unique functionality of line-based 4D printing for its self-locking, self-deploying, line-sculpting, and compliant structural aspects.

Regarding shape memory materials for 4D printing, A-line utilizes a common thermoplastic (PLA) that is widely used as a heat triggering shape-changing material. Among the most relevant previous work, Thermorph [1] achieved morphing interfaces with two different types of thermoplastic (PLA and TPU); Printed Paper Actuator [34] and Foldio [22] combined a single thermoplastic with other materials (e.g., paper, tape) to generate interactive objects. Using only one thermoplastic, Thunis Manen et al. presented a method which could morph a 2D construct to a 3D shape based on designing the printing path [33], yet that work does not account for angle control; 4DMesh [35] provided an inverse design tool to develop furniture-size mesh structures from arbitrary surfaces, yet the direction of each beam/line in their meshes was not controlled. A-line improves on these relevant projects by developing a design tool with accurate angle and direction control to open a new design space to achieve 4D-printed morphing structures from 1D (i.e., linear components) to 3D by using shape memory thermoplastics and FDM printers.

Programming Line-shaped Interfaces

In the field of HCI, researchers have proposed various line-shaped interfaces. LineFORM [21] and ChainFORM [20] explored an interaction design space with skeleton based actuation. As a soft and light actuation technique, PneUI [41] developed curling transformations with a pneumatic method.

Beyond the field of HCI, shape-changing lines have long been an area of active research. Daniel Cellucci et al. [2]

demonstrated a 1D printing system to create recyclable robots from a single string of source material. Skylar Tibbits [35] presented the idea of transforming lines using 3D printed multi-material lines. Weeger Oliver et al. [39] explored using multiple line segments to print 3D geometries that have heat-triggered shape memory effects. In the field of computer graphics, researchers introduced various systems to make aesthetically line-based objects, such as fashion design [9] and sculpture design [16].

Another relevant work is 4D rods [6] which shares a common design vision with A-line as both are heat-triggering programmed linear structures into 3D structures. Nevertheless, there are several differences between both projects. Firstly, 4D rods uses high-end PolyJet 3D printers, and A-line uses desktop FDM printers; 4D rods is a dual-material (elastomer and glassy polymer) system, and A-line uses a single material. Lastly, the composite design of 4D rods is based on isogeometric collocation method [40], where a 3D model is voxelated for the droplet jetting process. This computational model can't be easily adapted to an FDM printer. In contrast, we developed a method of bending angle control that is suitable for the continuous extrusion printing.

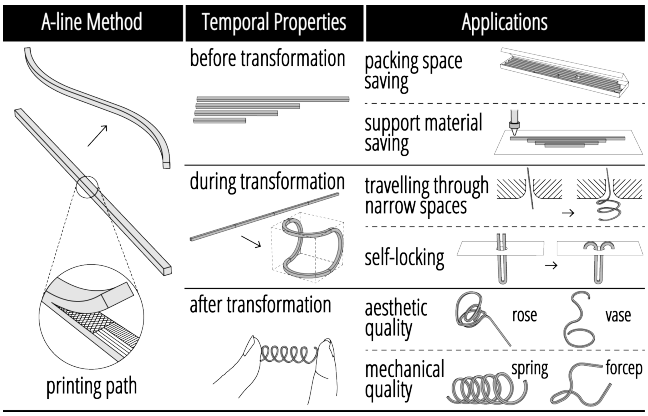

Figure 2: Design space of A-line.

4 A-LINE DESIGN SPACE

We hope the form factor of linear structures and the unique temporal transformation of A-line can open up new design spaces to the design and maker community (Figure 2). We identify A-line's linear components to have some unique properties following the temporal order: 1) before transformation, the compact 1D form factor; 2) during transformation, the transition in the space it consumes, and 3) post transformation, the unique aesthetic and mechanical quality.

The temporal properties of A-line can inspire applications in various contexts:

- self-deployable and self-locking structures in a constrained space: we demonstrate how 3D structures can self-assemble after passing through a narrow space (e.g., a hole, pipe, or tunnel).
- compliant mechanisms leveraging the inherent elastic properties of printed thermoplastic: structural components including springs, knots, twisting ties, and clips.
- line sculpting with the unique aesthetic quality of linear forms.
- reducing print time and support materials for 3D line forms: A-line divides a target 3D line structure into segments that are packed on the plane of the printing platform, eliminating the time required to print supporting structures in 3D space.

5 A-LINE METHOD

The initial geometry of A-line segments can be categorized into two classes- (1) a straight line composed of one or more linearly connected active segments and (2) multiple active segments joined together with passive segments. The passive segments can be either a straight line or a planar curve. Both active and passive segments share the same square cross-section throughout (Figure 3a). With the design tool, users can program the parameters of each individual segment, including length, bending angle, and bending direction.

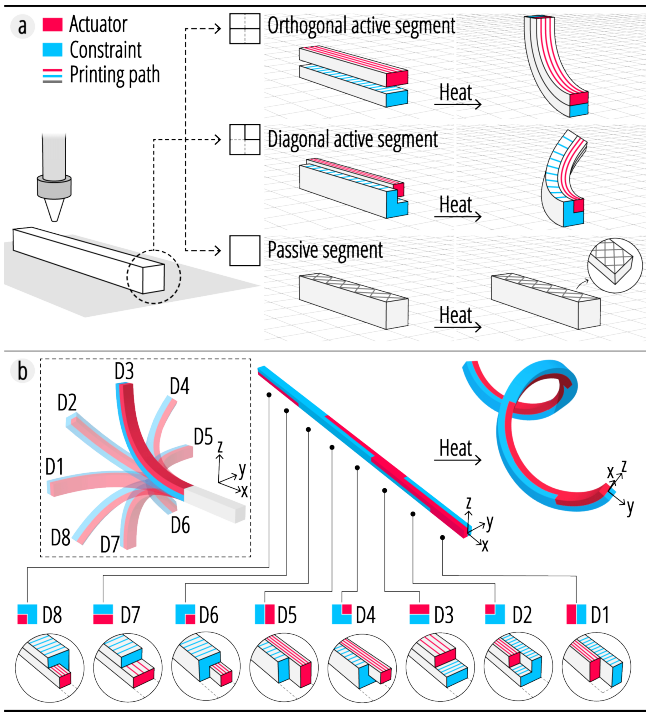

Figure 3: A-line structure. (a) Three types of segment composition; (b) Eight possible bending directions. By combining different bending directions for different segments, a straight line can transform into a helix with heat.

A-line is printed out of a single material- PLA (Polymaker PolyMax PLA) with a hobbyist desktop FDM 3D printer, and its bending direction and angle are controlled by changing the printing path. The lab ambient temperature is 20°-30°C and relative humidity is 30%-60%. Notably, PLA filaments will absorb moisture with prolonged exposure to open air and subsequently affect its printed quality. For this case, we store our filaments in contained boxes with silica gel desiccants.

Composite Design for Directional Bending Control

The key idea behind A-line is that a straight active line segment can have eight different potential bending directions. By combining multiple segments with varied bending directions, complex geometries can be fabricated (Figure 3b).

As preliminary studies [33] introduced and validated, PLA is observed to shrink along the printing direction. Different printing path direction within the linear segment would cause a difference in shrinkage rate, which allows the segment to self-bend when exposed to triggering forces. In the active segment, we propose an *orthogonal active segment* alongside with a *diagonal active segment* to enhance its capabilities of self-bending behavior (Figure 3a). In addition, we also bring in a *passive segment* for zero self-bending behavior.

Orthogonal Active Segment. Orthogonal bending actuators have been previously introduced [1, 35] and is one of the most commonly used morphing actuator structures. Our *orthogonal active segment* contains an actuator layer and a constraint layer (Figure 3a). This segment can be divided into two layers depending on the direction of the printing path. The parallel printing direction along the long edge of the linear segment, the actuator layer, results in the greatest relative shrinkage, whereas, printing direction perpendicular to the linear segment, the constrain layer, results in a relatively smaller shrinkage rate. When triggered, a segment composed of an orthogonal structure bends towards the actuator side due to its higher shrinkage rate.

Diagonal Active Segment. Similar to the *orthogonal active segment*, the *diagonal active segment* is also composed of actuator and constraint regions that are different in shrinkage rates. What is different in this structure is that in its cross-section, area centroids for actuator and constraint layers are not aligned orthogonally. Instead, they are positioned diagonally to facilitate 4 extra non-orthogonal bending directions (Figure 3a).

Passive Segment. Unlike the two active segments described above, the *passive segment* is used to minimize bending in any direction. We adopt a general cross printing path (Figure 3a) with a rectangular grid pattern of alternating printing angles (45° and −45°) to eliminate the differences in shrinkage rate and thus minimize the transformation.

Material Mechanism

We conducted a quantitative collection of the bending angle data for the active segments in relation to the actuator-constraint composition ratio and cross-section dimension.

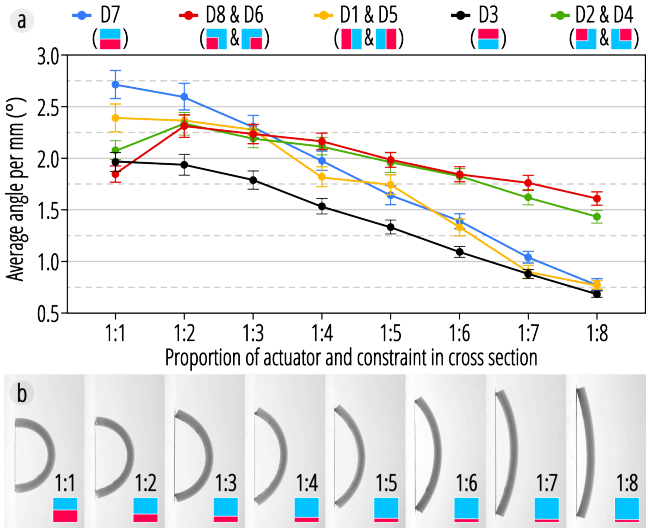

Figure 4: (a) Bending performances at eight directions. (b) Different ratios of the orthogonal active segment tested.

Bending Angle Control. Similar orthogonal segments have been quantified previously [35]. However, we conducted a new set of experiments for the following reasons: 1) in addition to the well-studied orthogonal toolpath alignment, we introduced diagonal alignment which could result in different bending performances; 2) different printing platforms and ranges of sample dimensions may affect performances.

We observed that the ratio between the cross-section area of two layers affects the bending angle of the active segments. To characterize this parameter, we experimentally printed eight ratios ranging from 1:1 to 1:8. Since some structural constructs are symmetric (e.g., D1 and D5 in Figure 3b) and have the same bending performance, we tested five of the possible eight bending directions. The size of the testing samples is 60 mm in length with a 4x4 mm cross-section area. In this experiment, we used a MakerBot Replicator 2X printing at speed 5000 mm/min, printing temperature 200°C, no printing bed heating, 0.1 mm layer thickness, with a 0.4 mm nozzle. Each setting was performed three times and averaged to minimize errors.

From the results, we observed that in orthogonal structures, the orthogonal ratio and bending angle demonstrates a roughly linear relationship, with the maximum bending angle occurring at 1:1 ratio (Figure 4). On the other hand, in diagonal structures, the maximum occurs at 1:2 ratio and the actuators contacting the print bed did not affect the performance significantly. Noticeably, the achievable ranges

of angles are different in each direction. These results are stored in our software implementation as references for a data-driven material programming.

Dimensionality. The thickness of segments also affects its bending performance. In our experiments, we investigated different dimensions of the cross sections from 1x1 mm to 6x6 mm for both a diagonal active segment and an orthogonal active segment. As Figure 5 shows, the smaller the cross-section area is, the bigger the bending curvature is.

Combining data collected from Figure 4 and Figure 5, we implemented four of the most reliable cross-section dimensions in our software: ranging from 1 mm to 4 mm cross-section dimension, with increments of 1 mm. Our experiments repeatedly showed that cross-section edge length smaller than 1mm is not feasible for achieving diagonal active segment due to the limited printing resolution, and a value larger than 4 mm provides bending curvatures that are too small for the scale of applications we are exploring. While we directly collected the bending curvature data for the sample with the cross section of 4x4 mm (Figure 4), the bending curvature for the other three cross-section dimensions are interpolated by combining the dimensional factor in Figure 5 and the bending performance of the 4x4 mm cross section samples shown in Figure 4.

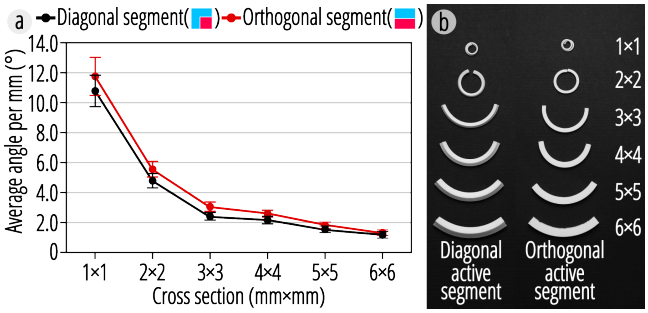

Figure 5: (a) The bending curvature decreases as the area size of the cross section increases; (b) The physical samples.

6 USER INTERFACE AND PIPELINE

A-line software uses Rhinoceros 6 as the design environment and Grasshopper as both a computational tool and an intermediary user interface. In general, the user workflow is: choose a library model or input a customized curve; define the number of segments and specify the length and actuation behavior for each segment; preview the transformation and generate the printing file.

User Workflow

Design the Basic Curve. Users can either choose an example curve from our library (Figure 6) or can import any planar curve drawn in Rhinoceros's environment. The samples in the library exemplify design primitives we used to generate more complex geometries. These examples provide previously designed passive segments, displayed in white, as well as editable active segments, displayed in red, that are initially set to certain bending and rotation angles to resemble some of our design examples. If users select one of the examples, they can extend the existing line with new active segments. If no library example is selected, users can design a standalone line with both passive and active segments from scratch in the Rhinoceros environment.

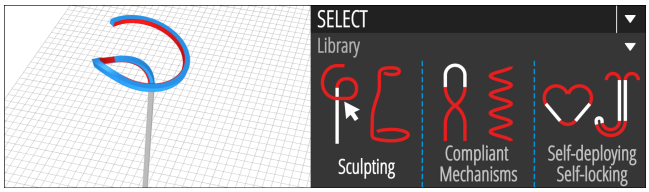

Figure 6: Choosing an example shape from a library.

Specify the Actuation Behavior. In this step, users can specify global variables such as segment width that apply to all available segments and can design the desired actuation behavior of each segment (Figure 7). At each segment, users can individually set the following variables to control simulated geometry: bending angles that defines the angle of each segment arc, bending direction that defines the relative rotation of the plane, and the length of each segment. With the help of the interpolation algorithm, users can modify these variables within the bounds of our data set to simulate estimated material behavior.

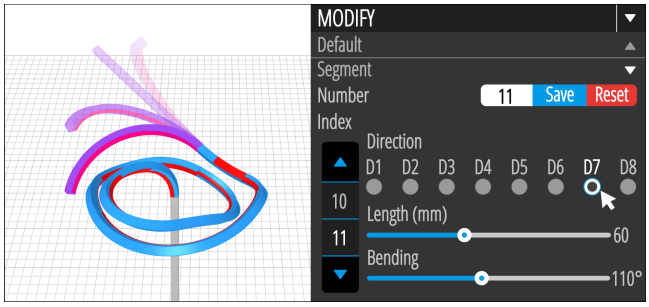

Figure 7: Segment-specific customization.

Fabrication Review and Simulation. The designed segments can be previewed in relation to the print bed (Figure 8b). If the designed line extends out of the print bed, the software will provide a warning sign. Users can split one continuous segment into shorter segments by specifying split indices. The software automatically reorients all segments in the print bed accordingly. In addition to the print bed review, users can also simulate the transformation of the line (Figure 8a). This way, the users can visually detect any obvious collisions and adjust the target shape to avoid them.

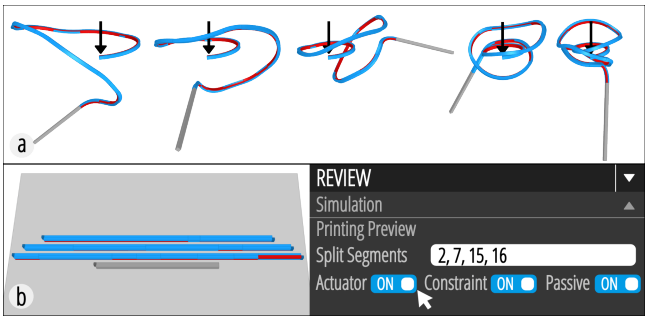

Figure 8: (a) Simulation. (b) Printing preview.

Export Printing Toolpaths and Post Processing. Lastly, users can input printer-specific parameters such as layer height, filament type, and nozzle diameters. When provided with these data, the software can automatically generate the toolpath for fabrication in the desired file directory. Once the G-code is saved, users can also preview line-based illustration of the toolpath within Rhinoceros environment. After printing, users can adhere the split segments with super glue then trigger them with heat (Figure 9).

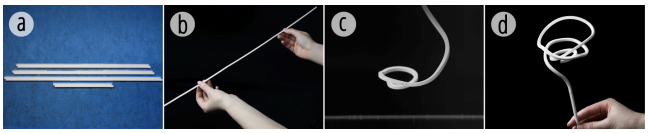

Figure 9: (a) Printed segments. (b) Assembly before triggering. (c) Triggering. (d) The final result.

Computational Pipeline

Data Interpolation. As the first step of integrating the directional bending behaviors of the material, we used a polynomial regression to interpolate data collected through physical material experiments in Figure 4. In addition to segment length and printing direction, our material tests showed us that another crucial parameter is the thickness of printed segments. We utilized polynomial regression function to estimate material behaviors at different thicknesses, by combining the comprehensive material testing at 4 mm thickness (Figure 4) and preliminary testing at 1, 2 and 3 mm thicknesses (Figure 5).

Geometric Abstraction of the Segments. To geometrically represent simulated bending segments, we simplify each segment into an arc (Figure 10a). In this abstraction, we assume that the curvature and the length of the segment are constant, neglecting insignificant warping and shrinking that is observed during the actuation. By calculating the effective radius of each actuated segment using user-defined bending angle and segment length, the geometric transformation can be represented computationally.

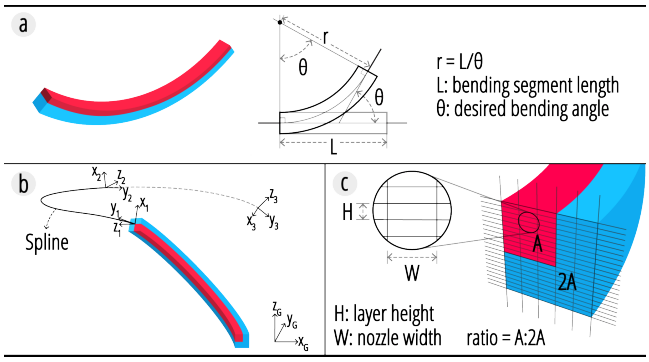

Figure 10: (a) Geometric abstraction of segment bending. (b) Geometric alignment of multiple segments. (c) Unit voxelization of the segment cross section to minimize floating point errors.

Modeling Multiple Segment Lines. Using the geometric abstraction discussed above, each segment arc is first generated in 2D according to user-defined bending angle and length. By evaluating perpendicular planes at the end and start of each arc, the software orients multiple segments to form a continuous spline (Figure 10b). By this point, the generated spline is planar. The algorithm then rotates the spline around Z axis of the corresponding plane with the user-defined relative rotation, resulting in a spline in 3D.

Voxel Division and 3D Segment Generation. We used another level of geometric reasoning to model each segment in 3D. Using the aforementioned data interpolation for each printing direction, we subdivide square cross section into actuator and constraint regions sized at the corresponding ratio. Dimensions of each actuator and constraint layers often result in decimal digits. Additionally, the printing resolution is constrained by the minimum layer height and nozzle width. Both factors could result in gaps between layers, overhangs, or poor adhesion between segments. To avoid floating point errors during G-code generation and fabrication steps, we rounded the dimension of each rectangular section along to Z axis to multiples of printing layer height, and along X and Y axes to multiples of the nozzle width (Figure 10c). These sections are then extruded along the segment curve to simulate actuated geometry.

Generating Fabrication Files. Having generated 3D geometries in previous steps, the software then flattens bent segments. At the end of each split segment, a passive notch is added to help combine multiple segments together after print. Then it lays-out divided pieces in an orthogonal direction to the print bed. Lastly, the software generates a printing path in constraint, actuator, or passive pattern, overlapping paths between conjoint segments to ensure better adhesion (Figure 11a).

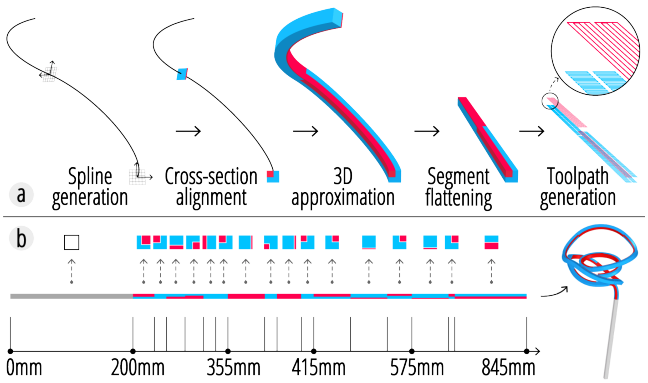

Figure 11: (a) Complete computational workflow. (b) The underlying linear structure can transform into a rose flower.

The tool is developed to empower users to design shapes that are hard to compute inversely. To demonstrate the complexity of the design that this tool can handle, Figure 11b reveals the underlying structure and parameters of the printed line that transformed into the rose.

7 TRIGGERING CONDITIONS

Hot Water as the Trigger

For our quantitative experiments and applications with a relatively high complexity, we follow the procedure described in the literature [35] and use hot water to trigger the artifacts shown in this paper (Figure 12). It provides uniform heating and high controllability with little gravitational effects hence has better accuracy and repeatability.

The fabricated pieces are submerged into 76°C hot water. It took around 1-2 minutes for the transformation to complete, but we wait until the water cools to 60°C to retrieve the samples after they are hardened. For most of the experiments except the springs leveraging gravitational forces, we added sugar into the water to increase its density to 1.16 g/mm^3 calibrated at the water temperature of 76°C to minimize the effect of gravity.

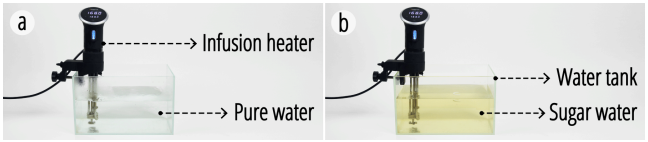

Figure 12: Water bath as the triggering condition.

Alternative Triggering Methods

Alternative triggering methods include heat gun, embedded resistive heating thread (e.g., carbon fiber), and hollow channels for steam. We have not quantified the accuracy of these triggering methods and recommend the uses of them for scenarios with low-accuracy requirements.

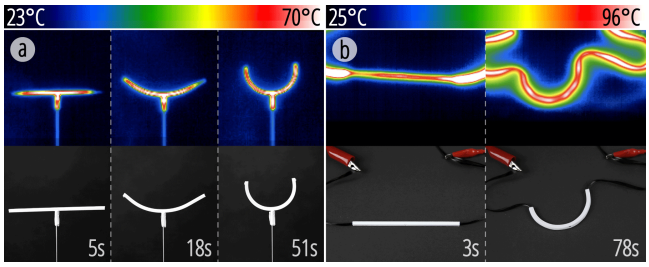

Figure 13: Photos and thermal images of the triggering process by steam (a) and heated carbon fiber (b) via resistive heating.

The benefit of using a heat gun is that users can selectively trigger the artifacts. On the other hand, the blowing wind may deform the objects undesirably depending on the artifact's scale. Internal heating methods also do not require the objects to be submerged into water, but they can be easily affected by gravity without buoyancy to compensate for its effect. The benefit of using steam channels or resistive heating fibers is that the triggering is embedded into the material structure. For these cases, we designed a hollow segment (Figure 13) which would either allow inserting resistive heating fibers (e.g., carbon fibers) or passing steam through the channel. The hollow channel is oriented along the segments, which do not affect the bending performance significantly but can accelerate transformations as heating the element is faster due to the increased surface area.

Serial and Parallel Transformation Behaviors

We can transform artifacts with either serial or parallel triggering. In this context, serial triggering refers to submerging the artifact following a certain sequence or order; and parallel triggering refers to submerging the entire artifact at once. The parallel triggering method provides a more uniform heating, for example, Figure 16c shows a vase triggered with this method.

However, there are two special cases when we recommend serial triggering by holding the artifact from one end and gradually submerging it into hot water. The intention is to avoid self-entanglement. For relatively long pieces, segments will transform concurrently and might curl to opposing directions, resulting in collisions and distortions. Serial triggering can circumvent this. As an example, Figure 14 shows the serial triggering process for the rose in Figure 9.

Figure 14: Serial triggering of a rose.

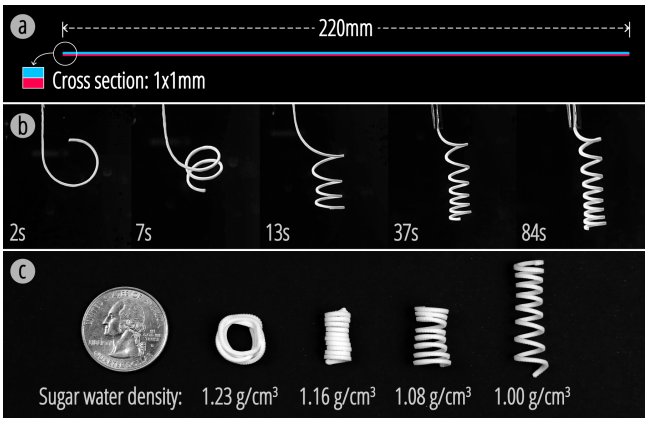

Figure 15: (a) An orthogonal active line segment. (b) The serial triggering process. (c) The effect of dissolved sugar concentration on the pitch of the spring.

Another important use case of the serial triggering method is to fabricate spring with various pitches. In particular, helixes with very small pitches cannot be achieved by the way in which A-line software would have been used to design a spring (i.e., implemented eight directions limit the pitch relative to the helix radius). With this sequential triggering method, the line is designed with uniform bending behavior towards a single direction along the artifact. If we leverage the gravitational effect by using pure water as a trigger, the heavier bottom will drop downwards rather than stay on the same lateral plane. With this procedural triggering, we can achieve a spring (Figure 15a and b).

Additionally, we can adjust the pitches of the spring by altering the density of water by adding sugar to modulate gravitational effects during transformations. Figure 15c shows four spring structures of the same compositional structure triggered in different water density. As demonstrated, higher density allows for smaller pitch as the effect of gravity is greatly reduced. Since the gravitational effect has not been integrated into our design tool yet, we cannot design and simulate the spring in A-line software. However, the experiment in Figure 15 can provide some reference data to control the diameter and pitch of a spring formed with this approach.

8 APPLICATIONS

Sculpting of Line-based Structures

A-line provides designers and artists with a method to produce line-based artifacts. Users can interactively program the lengths, directions, and bending angles of segments, receive real-time feedback on the transformations and resulting shapes, and rapidly iterate designs. Using our implementation, we designed a rose flower (Figure 9), a set of parametric vases of unique aesthetics (Figure 16a), and a skeleton for LED light stripes (Figure 16b).

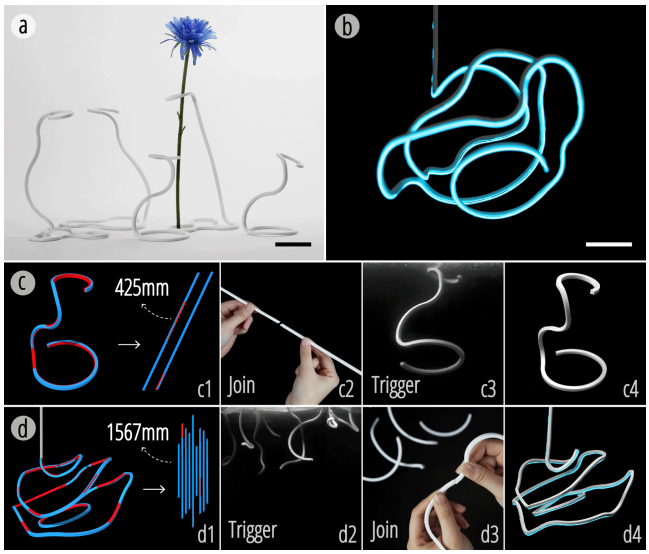

Figure 16: Vases and lamp. Scale bar: 50mm

Here we chose the vase and lamp as they exemplify various dimensional scales and triggering techniques. General conclusions can be drawn from these examples to inform selection of the most proper triggering strategy:

- small length: for lines with the length ranging from 10 cm to 50 cm (e.g., the vases in Figure 16c), segments can be joined together with super glue before the triggering, and simple parallel triggering method can be used.
- large length: for lines longer than 50 cm (e.g., the lamp in Figure 16d), the bending curvature variations are relatively big and collisions are very likely to happen. We recommend triggering individual segments separately in a parallel process before joining them together.

Compliant Mechanisms of Line-based Structures

A-line has a rich space for designing line-based compliant mechanisms in 3D. Compliant structures like twisting ties and springs are often difficult to make with an FDM printer as the object may fracture at the layering seams, and the support materials are hard to remove as the thin-line form factors make the whole structure fragile. Printing these objects with our techniques, the springs require no support and the seams are aligned with the curved structure and thus difficult to break. Leveraging these benefits, we designed a few compliant mechanism structures including twisting ties, springs, forceps, hairpins, knots, and clips. All examples shown in Figure 17 are transformed from straight lines.

Figure 18 shows a jumping toy with legs made of morphing variable springs. This is an extensive example of the spring discussed in Figure 15, with the serial triggering approach in pure water discussed earlier.

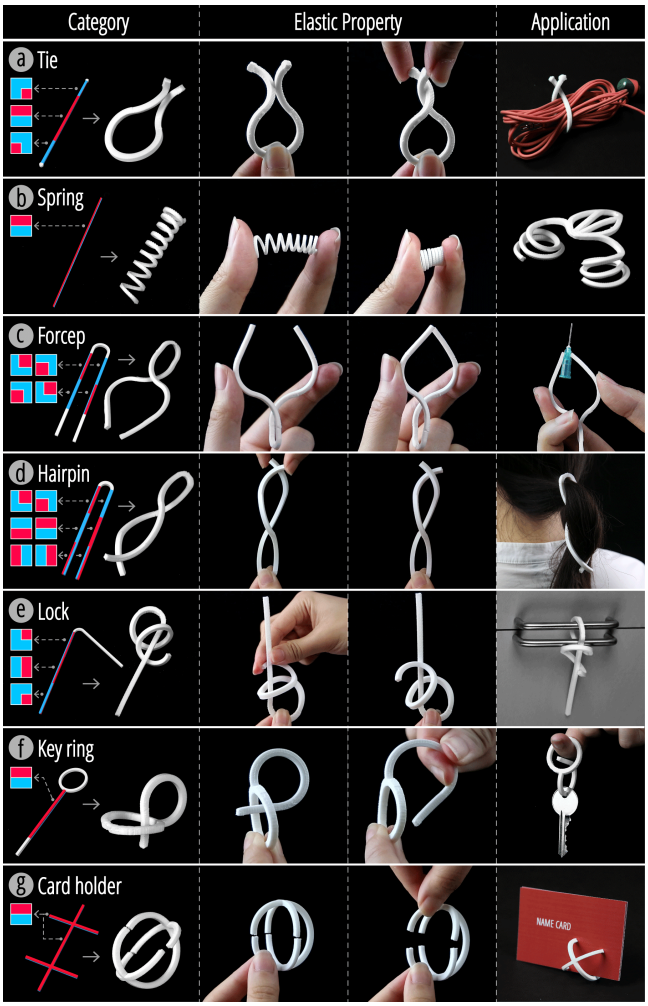

Figure 17: Various compliant mechanisms.

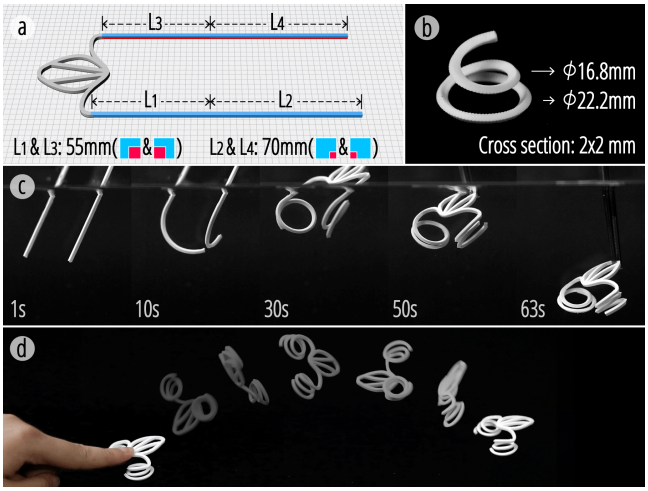

Figure 18: (a) The composition of a frog. (b) A variable spring designed as the bouncing leg. (c) Triggering. (d) Jumping.

Figure 19: (a) A wishing bottle. (b) A self-deploying hook.

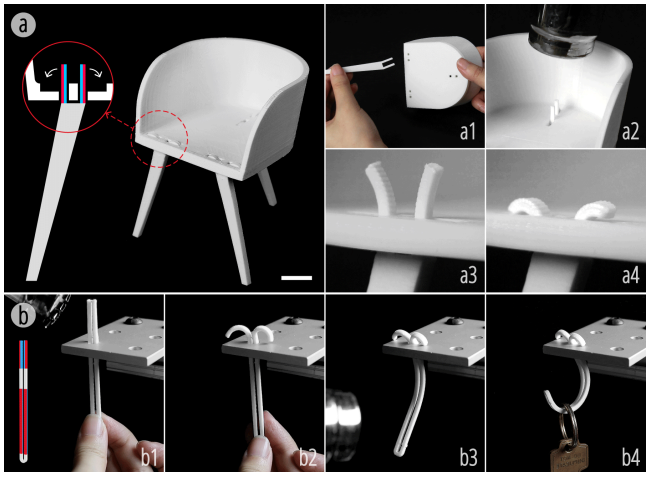

Figure 20: (a) A self-locking fixture. (b) A self-locking hook. Scale bar: 20mm.

Self-deployable and Self-locking Structures

One of the advantages of linear structures is that they can enter places where ordinary structures cannot reach, and then trigger its deformation for specific requirement (e.g., self-deployment and self-locking on site).

To demonstrate the self-deployment, we designed a wishing bottle that contains heart shapes that were placed through the narrow bottle neck when they were straight lines (Figure 19a). Figure 19b is an additional demo showing how a straight line can travel through a narrow space. As it self-folds into a variable spring hook, it captures the plastic. Afterwards, the spring hook can be quickly pulled out together with the plastic when it is still warm and deformable.

Additionally, to demonstrate the self-locking behavior, we showed chair legs that have self-locking fixtures, which can be triggered by heat (Figure 20a). We envision that such

fixtures can potentially save assembly effort and improve material recyclability by making the chair out of a single material without glue. The chair model has a scaling factor of 5.6. Taking the compressive strength of PLA as 2600 PSI, the calculated maximum load of the four legs in a 1:1 scaled model is robust enough to afford sitting. Figure 20b shows another self-locking example that can travel through a narrow hole and self-lock itself in place.

9 LIMITATION, DISCUSSION AND FUTURE WORK

Geometry and Accuracy

Bending Angles. A-line achieves eight bending directions in 3D space, and each direction can achieve a bending angle of 2-6 degree per mm. This means we can make a complex line-based shape, but not a completely arbitrary one.

Line Thickness. A-line supports four segment thickness scales and it requires that the thickness remains constant along the line. Additionally, the performance results and suggestions regarding the triggering conditions may not hold if dimensions are changed.

Length Factor. In A-line, we assume that the bending curvature is constant for a settled actuator-to-constraint ratio, and the accumulated bending angle increases proportionally as the length of the segment increases. This is generally the way literature treats thermoplastic-based 4D printing [1, 6]. However, our preliminary experiment shows that the length of the segment indeed affects the bending curvature. For example, an orthogonal active segment can increase its bending angle per mm from 1.5 to 2.5 degrees when the sample length is increased from 20 to 100 mm. This is a complex phenomenon involves different levels of stress release dynamics depending on its length, which requires further study.

Physical Forces. There are many internal and external forces that affect the transformation. In the software, the bending performance is based on data measured from an independent short beam. In the actual triggering process, adjacent segments may affect each other with torsional forces; gravity and water buoyancy may also affect the transformation. Even though we use sugar water to alleviate this effect, it is not optimal as the density of A-line structure changes slightly as it is being softened. To achieve a higher accuracy, future work may involve Finite Element Analysis for simulation and iterative optimization.

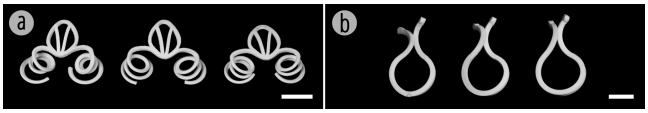

Figure 21: (a) The frogs through serial triggering. (b) The twisting ties through parallel triggering. Scale bar: 20mm.

Repeatability. A-line has good repeatability as long as the triggering condition stays consistent. Figure 21 shows the same structure printed three times. It shows serial triggering has a lower repeatability comparing with parallel triggering due to its manual feeding speed variations.

Software Improvements

Compared to the design software provided by related 4D printing works (e.g., Thermorph [1]), A-line provides only a forward design tool for line-based structures. An inverse design tool that can take a target shape or surface as input and flatten it to produce fabrication files is not included but also desired.

Hybrid Designs

While our software presents the design of A-line as standalone linear objects, we can combine it with surfaces and volumes to broaden our design space. Additionally, the voxelization design method and the software are adaptable to other morphing materials with adjustments/calibration. We can potentially incorporate multiple materials in one design to respond to different stimuli with distinct behaviors.

Envisioning Potential Design Spaces

In addition to the applications presented in this paper, A-line inspires us to think about novel application scenarios for line-based 4D printing. For instance, by replacing PLA with electrical field responsive hydrogels, surgeons could deliver a biocompatible line capable of moving through narrow spaces in the body and remotely transforming into a surgical tweezer on-site; through control of electrical field, remote control of the tweezer movement might be possible as well. In short, A-line will better motivate users to think about the multi-dimensionalities of 4D printing, and explore a myriad of bigger design spaces through life - interfaces that we use, play with, enjoy, live in, etc.

10 CONCLUSION

In this paper, we present A-line as an integrated printing and design method to morph a single linear element into a 3D line-based structure. Through this work, we hope to enlarge the design space of 4D printing technology. We encourage designers to think about novel uses of A-line in various aspects, including 1) the unique aesthetic quality of linear structures; 2) the unique flexibility of compliant structures; 3) the capability of 1D form to travel through narrow channels and self-deploy on site and 4) the inherent advantage of flat-packing for 4D printed artifacts. As for the next step, the computational design method can be generalized for other morphing materials or line-based materials as well, we hope the designer and maker community can carry the technique further to expand the design space of this method.

ACKNOWLEDGMENTS

This research was supported by the Carnegie Mellon University Manufacturing Futures Initiative, which was made possible by the Richard King Mellon Foundation.

The authors would also like to thank Lea Albaugh, Michael Rivera, Xiang 'Anthony' Chen, Youngwook Do, and Jianxun Cui for their constructive criticism; Jianzhe Gu and Zeyu Yan for assisting the preliminary experiments; Chengyuan Wei and Jack Forman for their conceptual ideas; Danli Luo for the linguistics suggestion; and Koya Narumi for the camera ready format support.

REFERENCES

[1] Byoungkwon An, Ye Tao, Jianzhe Gu, Tingyu Cheng, Xiang'Anthony' Chen, Xiaoxiao Zhang, Wei Zhao, Youngwook Do, Shigeo Takahashi, Hsiang-Yun Wu, et al. 2018. Thermorph: Democratizing 4D Printing of Self-Folding Materials and Interfaces. In *Proceedings of the 2018 CHI Conference on Human Factors in Computing Systems*. ACM, 260.

[2] Daniel Cellucci, Robert MacCurdy, Hod Lipson, and Sebastian Risi. 2017. 1D printing of recyclable robots. *IEEE Robotics and Automation Letters* 2, 4 (2017), 1964–1971.

[3] Xiang'Anthony' Chen, Stelian Coros, and Scott E Hudson. 2018. Medley: A Library of Embeddables to Explore Rich Material Properties for 3D Printed Objects. In *Proceedings of the 2018 CHI Conference on Human Factors in Computing Systems*. ACM, 162.

[4] Xiang'Anthony' Chen, Ye Tao, Guanyun Wang, Runchang Kang, Tovi Grossman, Stelian Coros, and Scott E Hudson. 2018. Forte: User-Driven Generative Design. In *Proceedings of the 2018 CHI Conference on Human Factors in Computing Systems*. ACM, 496.

[5] Kenneth C Cheung, Erik D Demaine, Jonathan R Bachrach, and Saul Griffith. 2011. Programmable assembly with universally foldable strings (moteins). *IEEE Transactions on Robotics* 27, 4 (2011), 718–729.

[6] Zhen Ding, Oliver Weeger, H Jerry Qi, and Martin L Dunn. 2018. 4D rods: 3D structures via programmable 1D composite rods. *Materials & Design* 137 (2018), 256–265.

[7] Christopher M Dobson. 2003. Protein folding and misfolding. *Nature* 426, 6968 (2003), 884.

[8] Scott E Hudson. 2014. Printing teddy bears: a technique for 3D printing of soft interactive objects. In *Proceedings of the SIGCHI Conference on Human Factors in Computing Systems*. ACM, 459–468.

[9] Emmanuel Iarussi, Wilmot Li, and Adrien Bousseau. 2015. WrapIt: computer-assisted crafting of wire wrapped jewelry. *ACM Transactions on Graphics (TOG)* 34, 6 (2015), 221.

[10] Alexandra Ion, Johannes Frohnhofen, Ludwig Wall, Robert Kovacs, Mirela Alistar, Jack Lindsay, Pedro Lopes, Hsiang-Ting Chen, and Patrick Baudisch. 2016. Metamaterial mechanisms. In *Proceedings of the 29th Annual Symposium on User Interface Software and Technology*. ACM, 529–539.

[11] Alexandra Ion, Robert Kovacs, Oliver S Schneider, Pedro Lopes, and Patrick Baudisch. 2018. Metamaterial Textures. In *Proceedings of the 2018 CHI Conference on Human Factors in Computing Systems*. ACM, 336.

[12] Alexandra Ion, Ludwig Wall, Robert Kovacs, and Patrick Baudisch. 2017. Digital mechanical metamaterials. In *Proceedings of the 2017 CHI Conference on Human Factors in Computing Systems*. ACM, 977–988.

[13] Gierad Laput, Xiang'Anthony' Chen, and Chris Harrison. 2015. 3D printed hair: Fused deposition modeling of soft strands, fibers, and bristles. In *Proceedings of the 28th Annual ACM Symposium on User Interface Software & Technology*. ACM, 593–597.

[14] Shiran Magrisso, Moran Mizrahi, and Amit Zoran. 2018. Digital Joinery For Hybrid Carpentry. In *Proceedings of the 2018 CHI Conference on Human Factors in Computing Systems*. ACM, 167.

[15] Vittorio Megaro, Jonas Zehnder, Moritz Bächer, Stelian Coros, Markus H Gross, and Bernhard Thomaszewski. 2017. A computational design tool for compliant mechanisms. *ACM Trans. Graph.* 36, 4 (2017), 82–1.

[16] Eder Miguel, Mathias Lepoutre, and Bernd Bickel. 2016. Computational design of stable planar-rod structures. *ACM Transactions on Graphics (TOG)* 35, 4 (2016), 86.

[17] Farhang Momeni, Xun Liu, Jun Ni, et al. 2017. A review of 4D printing. *Materials & Design* 122 (2017), 42–79.

[18] Stefanie Mueller, Sangha Im, Serafima Gurevich, Alexander Teibrich, Lisa Pfisterer, François Guimbretière, and Patrick Baudisch. 2014. WirePrint: 3D printed previews for fast prototyping. In *Proceedings of the 27th annual ACM symposium on User interface software and technology*. ACM, 273–280.

[19] Troy Robert Nachtigall, Oscar Tomico, Ron Wakkary, Stephan Wensveen, Pauline van Dongen, and Leonie Tentoff van Norten. 2018. Towards Ultra Personalized 4D Printed Shoes. In *Extended Abstracts of the 2018 CHI Conference on Human Factors in Computing Systems*. ACM, CS20.

[20] Ken Nakagaki, Artem Dementyev, Sean Follmer, Joseph A Paradiso, and Hiroshi Ishii. 2016. Chainform: A linear integrated modular hardware system for shape changing interfaces. In *Proceedings of the 29th Annual Symposium on User Interface Software and Technology*. ACM, 87–96.

[21] Ken Nakagaki, Sean Follmer, and Hiroshi Ishii. 2015. Lineform: Actuated curve interfaces for display, interaction, and constraint. In *Proceedings of the 28th Annual ACM Symposium on User Interface Software & Technology*. ACM, 333–339.

[22] Simon Olberding, Sergio Soto Ortega, Klaus Hildebrandt, and Jürgen Steimle. 2015. Foldio: Digital fabrication of interactive and shape-changing objects with foldable printed electronics. In *Proceedings of the 28th Annual ACM Symposium on User Interface Software & Technology*. ACM, 223–232.

[23] Jifei Ou, Gershon Dublon, Chin-Yi Cheng, Felix Heibeck, Karl Willis, and Hiroshi Ishii. 2016. Cilllia: 3D printed micro-pillar structures for surface texture, actuation and sensing. In *Proceedings of the 2016 CHI Conference on Human Factors in Computing Systems*. ACM, 5753–5764.

[24] Huaishu Peng, Jimmy Briggs, Cheng-Yao Wang, Kevin Guo, Joseph Kider, Stefanie Mueller, Patrick Baudisch, and François Guimbretière. 2018. RoMA: Interactive Fabrication with Augmented Reality and a Robotic 3D Printer. In *Proceedings of the 2018 CHI Conference on Human Factors in Computing Systems*. ACM, 579.

[25] Huaishu Peng, Jennifer Mankoff, Scott E Hudson, and James McCann. 2015. A layered fabric 3D printer for soft interactive objects. In *Proceedings of the 33rd Annual ACM Conference on Human Factors in Computing Systems*. ACM, 1789–1798.

[26] Huaishu Peng, Amit Zoran, and François V Guimbretière. 2015. D-coil: A hands-on approach to digital 3D models design. In *Proceedings of the 33rd Annual ACM Conference on Human Factors in Computing Systems*. ACM, 1807–1815.

[27] Parinya Punpongsanon, Xin Wen, David S Kim, and Stefanie Mueller. 2018. ColorMod: Recoloring 3D Printed Objects using Photochromic Inks. In *Proceedings of the 2018 CHI Conference on Human Factors in Computing Systems*. ACM, 213.

[28] Christina L Randall, Evin Gultepe, and David H Gracias. 2012. Self-folding devices and materials for biomedical applications. *Trends in biotechnology* 30, 3 (2012), 138–146.

[29] Dan Raviv, Wei Zhao, Carrie McKnelly, Athina Papadopoulou, Achuta Kadambi, Boxin Shi, Shai Hirsch, Daniel Dikovsky, Michael Zyracki,

Carlos Olguin, et al. 2014. Active printed materials for complex self-evolving deformations. *Scientific reports* 4 (2014), 7422.

[30] Michael L Rivera, Melissa Moukperian, Daniel Ashbrook, Jennifer Mankoff, and Scott E Hudson. 2017. Stretching the bounds of 3D printing with embedded textiles. In *Proceedings of the 2017 CHI Conference on Human Factors in Computing Systems*. ACM, 497–508.

[31] Paul WK Rothemund. 2006. Folding DNA to create nanoscale shapes and patterns. *Nature* 440, 7082 (2006), 297.

[32] Skylar Tibbits. 2014. 4D printing: multi-material shape change. *Architectural Design* 84, 1 (2014), 116–121.

[33] Teunis van Manen, Shahram Janbaz, and Amir A Zadpoor. 2017. Programming 2D/3D shape-shifting with hobbyist 3D printers. *Materials Horizons* 4, 6 (2017), 1064–1069.

[34] Guanyun Wang, Tingyu Cheng, Youngwook Do, Humphrey Yang, Ye Tao, Jianzhe Gu, Byoungkwon An, and Lining Yao. 2018. Printed Paper Actuator: A Low-cost Reversible Actuation and Sensing Method for Shape Changing Interfaces. In *Proceedings of the 2018 CHI Conference on Human Factors in Computing Systems*. ACM, 569.

[35] Guanyun Wang, Humphrey Yang, Zeyu Yan, Nurcan Gecer Ulu, Ye Tao, Jianzhe Gu, Levent Burak Kara, and Lining Yao. 2018. 4DMesh: 4D Printing Morphing Non-Developable Mesh Surfaces. In *The 31st Annual ACM Symposium on User Interface Software and Technology*. ACM, 623–635.

[36] Guanyun Wang, Lining Yao, Wen Wang, Jifei Ou, Chin-Yi Cheng, and Hiroshi Ishii. 2015. xPrint: from design to fabrication for shape changing interfaces by printing solution materials. In *SIGGRAPH Asia 2015 Posters*. ACM, 7.

[37] Guanyun Wang, Lining Yao, Wen Wang, Jifei Ou, Chin-Yi Cheng, and Hiroshi Ishii. 2016. xPrint: A Modularized Liquid Printer for Smart Materials Deposition. In *Proceedings of the 2016 CHI Conference on Human Factors in Computing Systems*. ACM, 5743–5752.

[38] Wen Wang, Lining Yao, Teng Zhang, Chin-Yi Cheng, Daniel Levine, and Hiroshi Ishii. 2017. Transformative Appetite: Shape-Changing Food Transforms from 2D to 3D by Water Interaction through Cooking. In *Proceedings of the 2017 CHI Conference on Human Factors in Computing Systems*. ACM, 6123–6132.

[39] Oliver Weeger, Yue Sheng Benjamin Kang, Sai-Kit Yeung, and Martin L Dunn. 2016. Optimal design and manufacture of active rod structures with spatially variable materials. *3D Printing and Additive Manufacturing* 3, 4 (2016), 204–215.

[40] Oliver Weeger, Sai-Kit Yeung, and Martin L Dunn. 2017. Isogeometric collocation methods for Cosserat rods and rod structures. *Computer Methods in Applied Mechanics and Engineering* 316 (2017), 100–122.

[41] Lining Yao, Ryuma Niiyama, Jifei Ou, Sean Follmer, Clark Della Silva, and Hiroshi Ishii. 2013. PneUI: pneumatically actuated soft composite materials for shape changing interfaces. In *Proceedings of the 26th annual ACM symposium on User interface software and technology*. ACM, 13–22.

[42] Lining Yao, Jifei Ou, Chin-Yi Cheng, Helene Steiner, Wen Wang, Guanyun Wang, and Hiroshi Ishii. 2015. BioLogic: natto cells as nanoactuators for shape changing interfaces. In *Proceedings of the 33rd Annual ACM Conference on Human Factors in Computing Systems*. ACM, 1–10.

[43] Lining Yao, Jifei Ou, Guanyun Wang, Chin-Yi Cheng, Wen Wang, Helene Steiner, and Hiroshi Ishii. 2015. bioPrint: A liquid deposition printing system for natural actuators. *3D Printing and Additive Manufacturing* 2, 4 (2015), 168–179.

[44] Amit Zoran. 2013. Hybrid basketry: interweaving digital practice within contemporary craft. *Leonardo* 46, 4 (2013), 324–331.